Research on the Outdoor Wind Environment of Buildings under the Influence of Hills: The Beigushan Hill in Nanjing

Tian Haoran, Jin Xing, Niu Shengnan, Ma congchao
Affiliation: School of Architecture, Southeast University
Email: tian_haoran@seu.edu.cn

Abstract
In urban planning and architectural design, mountains in complex terrains significantly impact buildings' outdoor wind environments, but research on hill-building interactions remains limited. Taking Beigushan Hill in Nanjing as the research object, this study uses CFD simulation to comprehensively explore the effects of factors like mountain height, building height, and building canyons on outdoor average wind speeds around buildings. It finds that Beigushan's unique terrain forms a high-speed zone on its leeward side, with a hilltop speed-up effect significantly increasing wind speeds around leeward buildings. The interplay of various factors jointly shapes the wind environment. The results provide a scientific basis for architectural design and planning under complex terrain conditions.

Key words: Complex Terrain; Outdoor Wind Environment of Buildings; CFD Simulation

1 Introduction

In the field of urban planning and architectural design, the impact of complex terrains on the outdoor wind environment of buildings is of great significance. Mountains, as common complex terrains, interact with buildings, altering wind direction, wind speed distribution, and pressure changes in the wind field (Alavi et al., 2024; Talwar & Yuan, 2024), and exerting a significant influence on climate-adaptive planning (Guo et al., 2025; Sun et al., 2011), urban thermal-wind environment (Guo et al., 2023; Mei et al., 2025; Sun et al., 2011), natural ventilation of buildings (Lin et al., 2020), pollutant dispersion (Kim et al., 2001), and pedestrian-level wind conditions (Baş et al., 2024; Mittal et al., 2018). Therefore, studying the outdoor wind environment of buildings influenced by mountains can provide a scientific basis for practical engineering optimization and planning decisions.

Complex terrains can modify the dynamic characteristics of atmospheric flow and affect the distribution patterns of wind fields at different spatial resolutions. Taking Nanjing as an example, as shown in Table 1, common terrains include steep terrain, hilly terrain, and low-lying irregular terrain covered by the city (Talwar & Yuan, 2024). Numerous studies have delved into wind field simulations under complex terrain conditions. For instance, literatures (Mei et al., 2025; Kim et al., 2001; Min et al., 2024; Blocken et al., 2015; Conan et al., 2016) have strived to reveal the influencing mechanisms on the wind environment and proposed specific challenges and application directions respectively. Min Zhong and Minghui Lin conducted wind tunnel tests on low-rise buildings in mountainous terrains in coastal areas (Min et al., 2024) and successfully established wind-resistant design criteria for low-rise buildings in mountainous areas; Tanya Talwar and Chao Yuan focused on the natural terrain of high-density residential areas in Singapore and found that the terrain effect is more pronounced under buoyancy-driven conditions (Talwar & Yuan, 2024); Jae-Jin Kim et al. used a two-dimensional numerical model to clearly illustrate the influence laws of hill slopes, building layouts, and their interactions on airflows and pollutant dispersion (Kim et al., 2001).

However, existing research findings are largely confined to aspects such as wind speed profiles, turbulence characteristics, and pressure distributions. Due to the complexity of mountain structures, differences in wind tunnel setups, and the diversity of boundary condition settings, these studies are difficult to compare directly. More crucially, most of the previous research has focused on the impact of relatively high mountains on the wind environment of high-density buildings. There remains a significant research gap regarding the interaction and potential impact between relatively low - lying mountains and buildings, which urgently requires in - depth exploration.

Table 1. Common Terrain Characteristics in Human Settlements (Taking Nanjing as an Example)

Common Terrain Characteristics in Human Settlements	**Geographical Concept Definition**	**Examples in Nanjing**
Type I: Steep Terrain	Small mountain ranges generally with an altitude of less than 1000 meters and a relative height of > 200 meters	Such as Zijin Mountain, etc.
Type II: Hilly Terrain	Generally with an altitude of less than 1000 meters and a relative height of < 200 meters	Such as Fangshan Mountain, Mufu Mountain, etc.
Type III: Low - lying Irregular Terrain Covered by the City	Generally with an altitude of less than 100 meters, a relative height of 10 - 60 meters, and a ground slope of 5° - 15°	Such as Qingliang Mountain, Shijingshan Mountain, Beigushan Hill, etc.

This study focuses on the impact of low-lying mountains (hills) within urban building clusters on the average wind speed. Taking Beigushan Hill in Nanjing as an example, it deeply analyzes the influence of factors such as mountain height, building height, and building canyons on the outdoor wind environment of buildings. Section 2 will detail the computational settings and parameters of the numerical simulation; Section 3 will analyze the research results and discuss the role of each influencing factor; Section 4 will summarize the main findings and conclusions.

2. CFD Simulation: Computational Settings and Parameters

2.1 Computational Geometry, Domain, and Grid

The study area is located in Beigushan Hill, a southern branch of the Mufu Mountain range in the north of Nanjing City, Jiangsu Province, China. Its longitude and latitude range from 118° 47' 2.89" to 118° 47' 37.34" E and from 32° 6' 14.42" to 32° 6' 45.83" N, with a total area of 0.351 square kilometers. Nanjing is in the subtropical monsoon climate zone. Meteorological data required for this study, such as air properties, wind direction and speed, temperature, and humidity, are all sourced from the publicly available data of Jiangsu Meteorological Station. In the simulation, the wind direction is set as the dominant summer wind direction in Nanjing - the southeasterly monsoon (θ = 22.5°). The computational geometry of the mountain is constructed based on the digital elevation data with a spatial resolution of 30m provided by ASTER GDEM V3.

In this study, a multi-storey residential building model with a length of 40m × width of 12m × height of 24m was constructed to depict the spatial characteristics of the residential area around the mountain. The longitudinal spacing of all buildings is set at 32m, and the transverse spacing is 40m. This size layout strictly adheres to the requirements of the existing residential design code (Ministry of Housing and Urban-Rural Development of the People's Republic of China, 2018).

Based on this layout, the study further explores the influence of relevant factors such as mountain slope, building height, and building canyons on the wind environment. The specific parameter changes and model settings are detailed in Table 2.

Table 2. Parameter Changes and Model Settings

Parameter Changes	Model Settings
Basic Working Conditions	A1: Building height is 24m, mountain height is H
Changes in Mountain Height (Slope)	B1: Building cluster remains unchanged, mountain height is 0.5H B2: Building cluster remains unchanged, mountain height is 2H
Changes in Building Height	C1: Mountain remains unchanged, building height is 18m C2: Mountain remains unchanged, building height is 30m
Changes in Building Canyons	D1: Building orientation is perpendicular to the incoming wind D2: Building orientation is perpendicular to the incoming wind and arranged staggeredly D3: Based on A1, the building orientation remains unchanged, and the local building canyon morphology on the leeward side of the mountain is changed
Ideal Mountain	E1: Three sinusoidal - shaped mountain peaks, height is H

In the process of constructing the CFD simulation model, the modeling experience of existing CFD studies on complex terrains and urban forms [1, 12, 14-15] was drawn upon. As shown in Figure 1-a, the computational domain and boundary conditions were set following these principles: The inlet boundary and side boundaries were set at a distance of 30H (H is the mountain height) from the building cluster to ensure that the flow is fully developed and the side-boundary effect is eliminated before reaching the reference wind - measuring tower M0. The outlet boundary was set at a distance of 60H from the building cluster to ensure that the flow is fully developed in the wake region. The height of the computational domain is 12H. After calculation, the blockage ratio is in the range of 2.7-2.9, meeting the industry standard requirement of being less than 3%. The computational domain size and the number of meshes were effectively reduced through a working - condition-based modeling strategy. The computational domain was meshed with hexahedral meshes, and local refinement was carried out at the buildings and the mountain. The minimum mesh size is 5m, the maximum size is 50m, and the expansion coefficient of adjacent meshes is controlled at 1.2 (Figure 1-b). For different working - condition settings, the total number of meshes ranges from 1.6 million to 2 million cells, and the average mesh volume quality is greater than 87%.

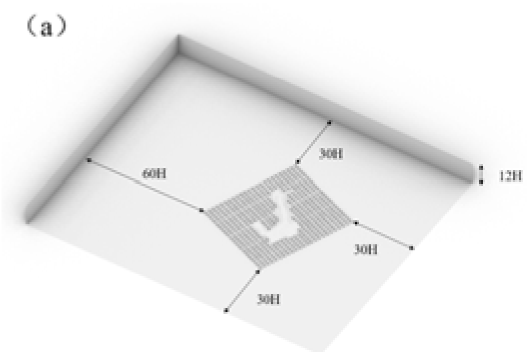

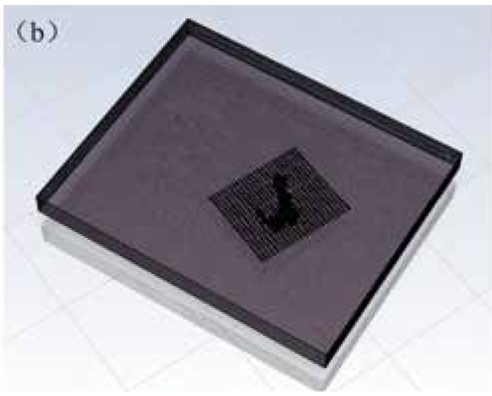

Figure 1. Computational Domain Setup (a) Size of the Computational Domain (b) Meshing and Local Refinement

2.2 Boundary Conditions and Solver Settings

At the inlet of the computational domain, the equations of Richards and Hoxey (1993) were used to impose the inlet profiles of the vertical wind speed profile U, turbulent kinetic energy k, and turbulent dissipation rate ε:

$$U(z) = \frac{U^*}{K} ln\left(\frac{z+z_0}{z_0}\right) \quad (1)$$

$$k(z) = \frac{U^{*2}}{\sqrt{C\mu}} \quad (2)$$

$$\varepsilon(z) = \frac{U^{*3}}{K(z+z_0)} \quad (3)$$

$$U^* = K\frac{U_{ref}}{\left(\frac{H_{ref}+z_0}{z_0}\right)} \quad (4)$$

where *K* is the von Karman constant, typically with a value between 0.40 ± 0.02. In this paper, the value is 0.42; *z* is the height at which the velocity is calculated (m); *Z(0)* is the aerodynamic roughness length (m), which varies depending on the landscape. In this paper, the value is 1 to represent a closed landscape, such as a mature forest, homogeneous city, and village; *Cμ* is the turbulent viscosity constant with a value of 0.09; *U** is the friction velocity, calculated by Equation (4), and the value is 0.49.

Symmetry boundary conditions were imposed on the top and sides of the domain. At the outlet boundary of the domain, a pressure - outlet condition was adopted. For the floor and building surfaces, a no - slip wall boundary condition was used. The commercial CFD code ANSYS/Fluent was used to solve the 3D steady-state Reynolds-Averaged Navier-Stokes (RANS) equations by means of the control volume method. The realizable k-Δmodel was selected to close the equations. For the convective and viscous terms of the governing equations, a second-order discretization scheme was employed. The pressure-velocity coupling adopted the COUPLED algorithm, and standard pressure interpolation was used. The simulation was run continuously until the residuals stabilized and reached a convergent state. Generally, the residual of the continuity equation is equal to or less than 10(-3), and the residuals of the velocity components \(k\) and \(\varepsilon\) are lower than 10(-5).

3. Results and Discussion

3.1 Influence of Beigushan Hill's Terrain on Wind Speed

Beigushan Hill has a unique terrain with four sub-peaks. As shown in Figure 2a, three distinct high-speed bands are generated on its leeward side. From the perspective of aerodynamic principles, due to their special terrain orientation and spatial positions, the northernmost and westernmost peaks have a more significant obstructive and guiding effect on the airflows compared to the two middle peaks, thus resulting in a more prominent acceleration effect on the leeward side. When only the mountain is present, according to the principle of flow around an object in aerodynamics, the mountain forms a shielding effect on the airflows on its leeward side, leading to a decrease in wind speed on the leeward side. However, when a low-height mountain is embedded in the building cluster, the hilltop wind-acceleration effect comes into play (Figure 2b). This effect stems from the fact that when the airflow passes over the hilltop, the streamlines are compressed. According to Bernoulli's principle, the flow velocity increases and the pressure decreases, creating a high-wind-speed zone around the leeward-side buildings in the wake region of the mountain peak. Quantified by data, under the condition of a pure building cluster without a mountain, the overall average wind speed in the study area is 0.552 m/s, which increases to 0.646 m/s when a mountain is present, with an increase of 17.04%.

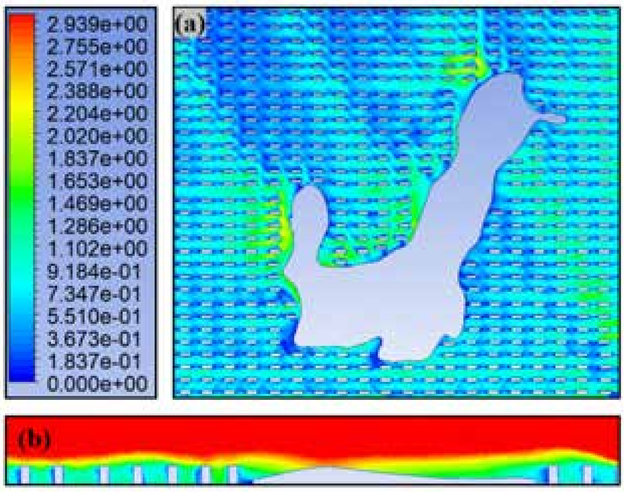

Figure 2. Wind Speed Results (m/s) for Basic Working Condition A1 (a) z=1.5m (b) y-z, x=1340m

For a uniform building array, as shown in Figure 3a, it exhibits a significant wind - blocking effect. The wind speed in the study area decays from 4-4.5 m/s in the free-stream to 0.5-1m/s, which is in line with the expectations of the Urban Canopy Model (UCM). It is worth noting that when the building cluster forms a specific angle with the incoming wind direction, due to the complex flow-around and wake-flow effects among the buildings, a high-wind-speed band will be formed in its wake region. This phenomenon should be avoided as much as possible in future experimental designs to prevent interference with the study of other factors.

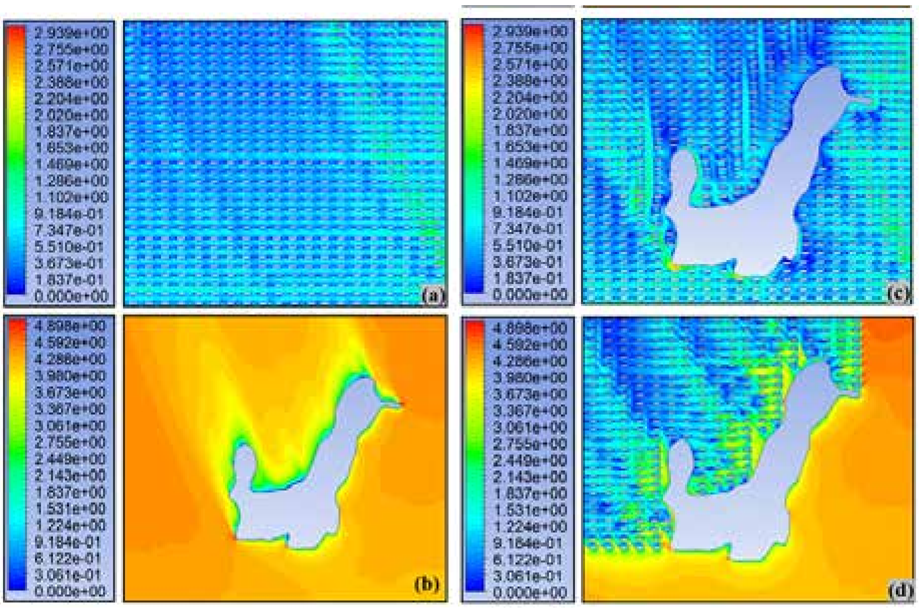

Figure 3. Wind Speed Results (m/s) for Model Validation (a) Wind speed at z=1.5m with only building clusters (no mountain) in the study area (b) Wind speed at z=1.5m with only the mountain (no building clusters) in the study area (c) Wind speed at z=1.5m when the mountain has no slope but a height of H (only mountain shape retained) (d) Wind speed at z=1.5m when buildings on the windward side of the mountain are removed

When only the mountain is present (Figure 3b), it shelters the leeward area. The windward region maintains free-stream wind speeds as it is undisturbed by buildings. On the leeward side, airflow is blocked by the mountain, causing separation and recirculation, reducing the average wind speed from 4-4.5 m/s (upwind) to 1-4 m/s—a 75% decrease from the free stream.

Although a deceleration zone also exists on the mountain's windward side, its size is smaller due to the relatively small windward surface and limited airflow obstruction, with an average wind speed reduction of only 0.5-1 m/s. Meanwhile, local high wind speed points form on both sides of the mountain due to flow-around and acceleration effects.

In scenarios where the mountain interacts with buildings (Figure 3c), corner flow acceleration and airflow separation mechanisms increase local wind speeds on the western side of the mountain. The accelerated airflow experiences a Venturi effect as it passes through mountain-building air ducts. Narrow channels formed by downstream building gaps further concentrate the airflow, creating a sustained high-speed zone.
Simulations with windward-side buildings removed (Figure 3d) still clearly show an acceleration zone on the mountain's leeward side with an unchanged spatial distribution trend. This confirms that the mountain's inherent topographic acceleration effects (e.g., hilltop acceleration, corner flow acceleration) are the primary drivers of the leeward acceleration zone. Without windward buildings to decelerate airflow, wind speeds behind the mountain are higher than in the basic case (A1, Figure 2a). Thus, windward buildings primarily affect local wind speed reduction and have limited impact on the airflow structure of the leeward side, while the leeward high-speed zone is driven mainly by terrain-building coupling effects (e.g., air duct acceleration, separation-reattachment flow).

3.2 Influence of Mountain Height on Hilltop Wind Acceleration Effect
There is a significant positive correlation between the hilltop wind acceleration effect and mountain height (Figure 2a; Figure 4a-b). When the mountain height is 0.5H (Figure 4a), the intensity and continuity of the high wind speed band on the leeward side are weaker compared to Case A1 (Figure 2a) at pedestrian level. This is because lower mountains have limited airflow acceleration capacity and cannot form stable or intense acceleration zones.

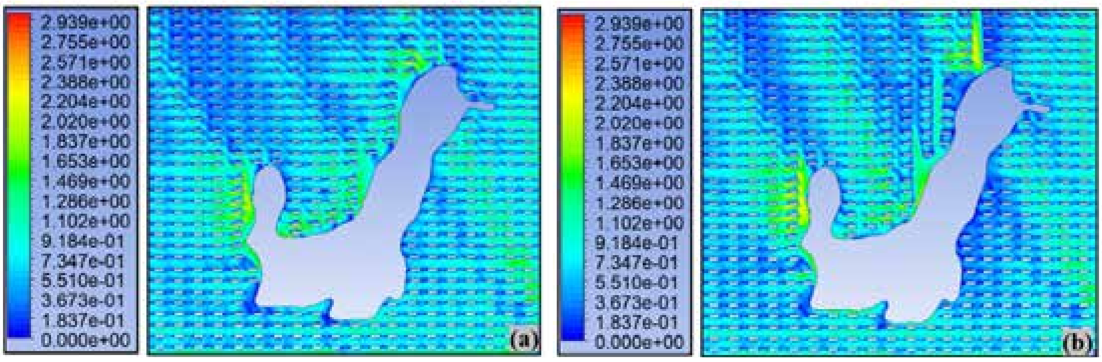

Figure 4. Wind Speed Results (m/s) for Mountains of Different Heights (a) C1 z=1.5m (b) C2 z=1.5m

When the mountain slope in B2 increases to 2H (Figure 4b), the wind speed increase at the hilltop becomes more pronounced, and the spatial continuity and intensity of the high wind speed band on the leeward side are enhanced. In the B1 case, even though the mountain height (18m) is lower than the building height (24m), according to the aerodynamic characteristics of airflow around obstacles of different heights, an acceleration zone on the leeward side of the mountain can still be observed, fully demonstrating that the acceleration effect exists even when the mountain is lower than the buildings.

3.3 Influence of Building Height on Wind Speed Distribution
When studying the influence of building height on wind speed, in C1, the building height is reduced to half of the mountain height (Figure 5a). The distribution trend of the high wind speed band on the leeward side of the mountain is the same as that in the basic working condition A1 (where the building height is 2/3H=24m), and the overall wind speed in the area increases. This is because lower buildings weaken the blocking effect on the airflow, increasing the overall wind speed. In C2, the building height is increased to be close to the mountain height (Figure 5b), and the intensity of the high wind speed band on the leeward side of the mountain increases slightly, but the effect is not significant.

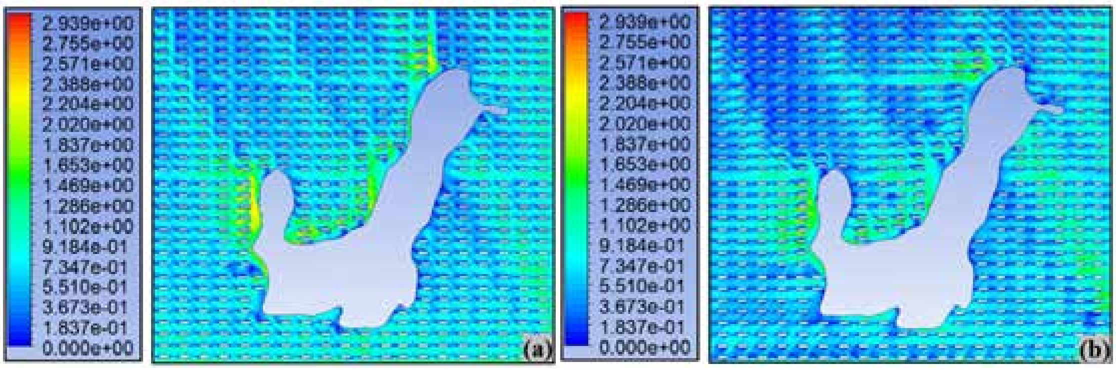

Figure 5. Wind Speed Results (m/s) for Buildings of Different Heights (a) C1, z=1.5m (b) C2, z=1.5m

Meanwhile, due to the enhanced building shielding effect, the overall wind speed in the area decreases, and the area of the calm wind zone increases. In the leeward building canyons, the continuity of the acceleration zone in C2 is significantly enhanced, with accelerated winds flowing westward; in the building canyons of C1, the accelerated winds flow northwestward. This difference may arise from the varying guidance and constraint effects of building canyons on airflow at different building heights.

3.4 Influence of Building Orientation on Wind Speed Distribution

In D1 and D2, the building orientation is changed to be perpendicular to the incoming wind direction. Under D2 conditions, where buildings are arranged in a staggered manner and there is no building canyon acceleration effect on the windward side of the mountain (dominated solely by the hilltop wind acceleration effect), the acceleration zone on the leeward side of the mountain is smaller, with a horizontal extension of approximately 4H (Figure 6b). Figure 6a clearly demonstrates the canyon acceleration effect of buildings: after the incoming wind is accelerated through the windward building canyons of the mountain and then further accelerated by the hilltop, the wind speed in the leeward building canyons reaches 3.5 m/s, significantly extending the length of the acceleration zone to a horizontal range of approximately 14H–26H. In areas without hilltop wind acceleration on both sides of the mountain, where the incoming wind is only accelerated by building canyons, the acceleration effect only persists for a short distance, and wind speeds around buildings farther from the velocity inlet tend to return to lower levels.

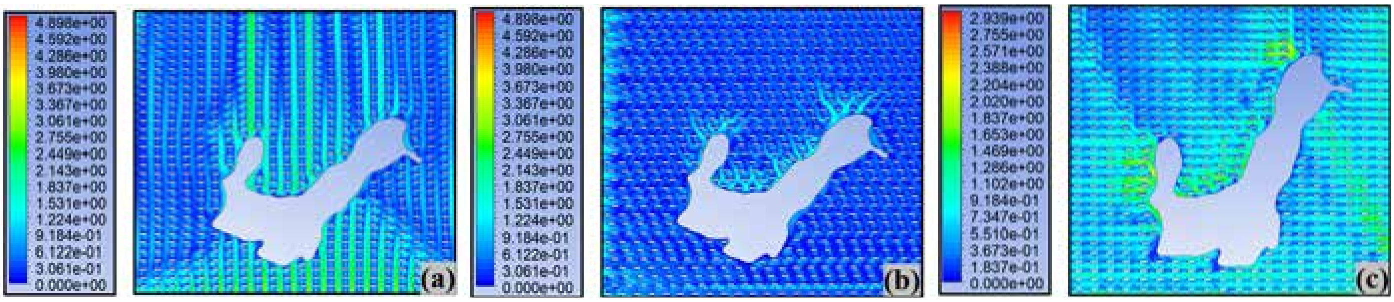

Figure 6. Wind Speed Results (m/s) for Modified Building Canyons (a) D1, z=1.5m (b) D2, z=1.5m (c) D3, z=1.5m

When the mountain and buildings form a continuous air duct, the acceleration zone extends significantly, clearly indicating that the high wind speed band on the leeward side is synergistically enhanced by the hilltop wind acceleration effect and the air duct effect (Figure 6c).

3.5 Comparison of Wind Speed Conditions Between Idealized Mountain and Standard Case

Three distinct high wind speed bands form on the leeward side of the idealized mountain, consistent with the trend observed in the standard case A1 (Figure 7a). Notably, the acceleration zone behind Peak 3 exhibits significantly higher wind speeds than those behind the other two peaks. This is because the incoming wind, pre - accelerated by the upstream buildings, is rapidly accelerated again by the hilltop, resulting in a synergistic effect that greatly enhances the acceleration (Figure 7).

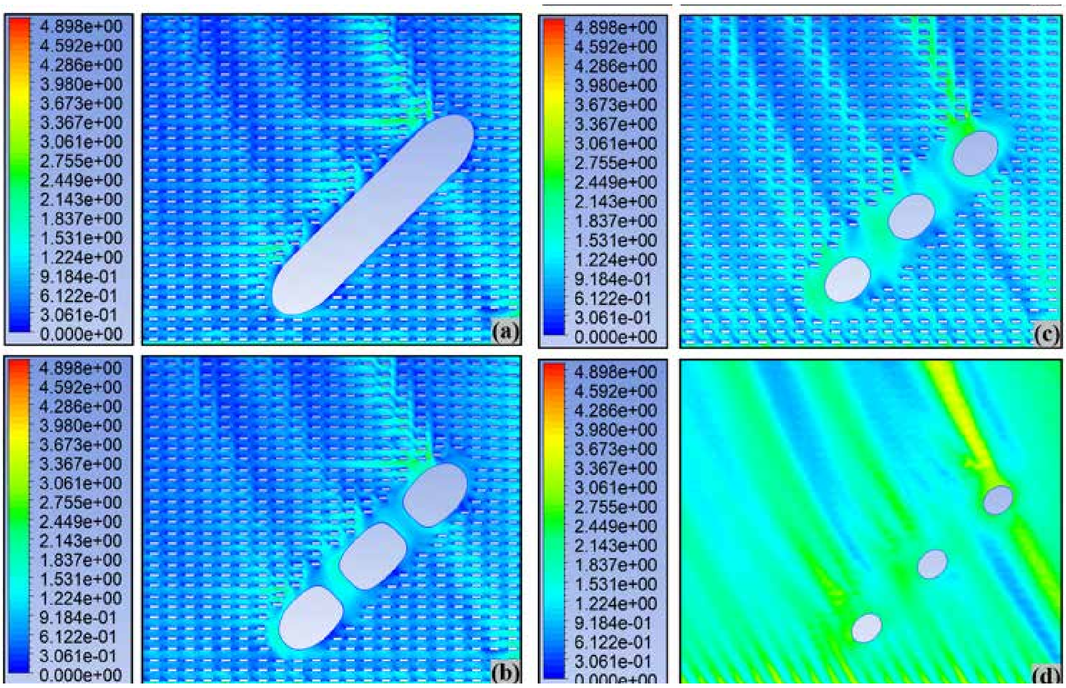

Figure 7. Wind Speed Results (m/s) for the Idealized Mountain (a) z =1.5m (b) z=10m (c) z=20m (d) z=30m

4. Conclusions

This study investigates the impact of low-lying mountains within urban building clusters on the surrounding pedestrian-level wind environment. An improved CFD model was used to simulate the urban wind environment, and the influence of multiple factors on the wind environment was analyzed by setting different working conditions. This paper provides a scientific basis for urban planning and architectural design optimization under complex terrain conditions, and lays a foundation for subsequent in-depth research on wind environments under different climatic conditions, more complex terrains, and multi - factor coupling effects, while offering technical references.

The specific research achievements and findings are as follows:

1. When a low-altitude mountain is embedded within a building cluster, the hilltop wind acceleration effect is significant. Compared with pure building conditions, this effect increases the wind speed around leeward buildings and forms high-wind-speed bands.

2. There is a significant positive correlation between mountain height and the hilltop wind acceleration effect. As the slope increases, the wind speed increase at the hilltop becomes more pronounced, and the spatial continuity and intensity of the high-wind-speed bands on the leeward side are enhanced. However, the acceleration effect still exists even when the mountain is lower than the buildings.

3. Changes in building height affect the high-wind-speed bands on the leeward side of the mountain and the overall wind speed in the area. The guiding and constraining effects of building canyons on airflows differ at different building heights.

4. When the leeward side of the mountain is dominated solely by the hilltop wind acceleration effect, the acceleration zone is small in scope. When the mountain and buildings form a continuous air duct, the acceleration zone extends significantly, indicating that the high-wind-speed bands on the leeward side are synergistically enhanced by the hilltop wind acceleration effect and the air duct effect.

In the field of architectural design and planning, the following series of valuable recommendations can be derived from the above research results, aiming to optimize building layouts and designs, improve wind environment quality, and enhance residential comfort and energy utilization efficiency:

1. Ventilative Building Layout: When planning building clusters, locate buildings with high ventilation requirements (such as hospitals and schools) in the high-wind-speed bands on the leeward side of low-altitude mountains to enhance natural ventilation through the hilltop wind acceleration effect.

2. Layout According to Mountain Height: Mountain architectural design should consider the relationship between mountain height and wind acceleration. The leeward side of high-slope mountains is suitable for installing wind power generation facilities. Meanwhile, building heights should be reasonably arranged to prevent excessive obstruction of airflows.

3. Optimized Building Canyon Design: Determine building heights according to functional and ventilation requirements. For example, in commercial pedestrian streets, adjust heights reasonably to guide airflows through building canyons and create a comfortable breeze environment.

4. Creation of Continuous Air Ducts: When planning large - scale building areas (such as residential communities), rationally design building orientations and layouts to form continuous air ducts between mountains and buildings, thereby promoting air circulation.

References

Alavi, F., Moosavi, A. A., Sameni, A., et al. (2024). Numerical simulation of wind flow characteristics over a large-scale complex terrain: A computational fluid dynamics (CFD) approach. *City and Environment Interactions*, 22, 100142.

Baş, H., Andrianne, T., & Reiter, S. (2024). City configurations to optimise pedestrian level ventilation and wind comfort. *Sustainable Cities and Society*, 114, 105745.

Blocken, B., Hout, D. V. A., Dekker, J., et al. (2015). CFD simulation of wind flow over natural complex terrain: Case study with validation by field measurements for Ria de Ferrol, Galicia, Spain. *Journal of Wind Engineering & Industrial Aerodynamics*, 147, 43–57.

Conan, B., Chaudhari, A., Aubrun, S., et al. (2016). Experimental and Numerical Modelling of Flow over Complex Terrain: The Bolund Hill. *Boundary-Layer Meteorology*, 158(2), 183–208.

Guo, Q. J., Lin, Y. Y., & Zhang, X. J. (2025). Identification and cooling effect analysis of urban ventilation corridors in coastal hilly cities: A case study of Shenzhen. *Urban Climate*, 61, 102393.

Guo, X., Yan, C., & Miao, S. (2023). A rapid modeling method for urban microscale meteorology and its applications. *Science China Earth Sciences*, 66(10), 2224–2238.

Kim, J., Baik, J., & Chun, H. (2001). Two-dimensional numerical modeling of flow and dispersion in the presence of hill and buildings. *Journal of Wind Engineering & Industrial Aerodynamics*, 89(10), 947–966.

Ju, P., Li, M., et al. (2022). Review of Research Advances in CFD Techniques for the Simulation of Urban Wind Environments. *Fluid Dynamics & Materials Processing*, 18(2), 449–462.

Lin, X. D., Wu, J., Mahroo, E., et al. (2020). Improvement Strategies Study for Outdoor Wind Environment in a University in Beijing Based on CFD Simulation. *Advances in Civil Engineering*, 2020, Article ID 8850340.

Mei, J. S., Hang, J., Fan, Y., et al. (2025). CFD simulations on the wind and thermal environment in urban areas with complex terrain under calm conditions. *Sustainable Cities and Society*, 118, 106022.

Min, Z., Minghui, L., Zhanxue, Z., et al. (2024). Wind tunnel test on low-rise buildings influenced by hillside height in typical mountain terrain. *Advances in Aerodynamics*, 6(1), Article ID 9489326.

Mittal, H., Sharma, A., & Gairola, A. (2018). A review on the study of urban wind at the pedestrian level around buildings. *Journal of Building Engineering*, 18, 154–163.

Sun, L., Nottrott, A., & Kleissl, J. (2011). Effect of hilly urban morphology on dispersion in the urban boundary layer. *Building and Environment*, 48, 195–205.

Talwar, T., & Yuan, C. (2024). Impact of natural urban terrain on the pedestrian wind environment in neighborhoods: A CFD study with both wind and buoyancy-driven scenarios. *Building and Environment*, 261, 111746.

You, W., & Liang, Y. (2024). Numerical investigation of different building configurations for improving outdoor spatial ventilation conditions in strip-type residential neighbourhoods. *Urban Climate*, 56, 102012.